Surface Science 602 (2008) 2206–2211

Contents lists available at ScienceDirect

Surface Science

journal homepage: www.elsevier.com/locate/susc

DFT study of methanol adsorption and dissociation on β-Mo_2C(001)

C. Pistonesi [a], A. Juan [a,*], A.P. Farkas [b], F. Solymosi [b]

[a] Departamento de Física, Universidad Nacional del Sur, Avda. Alem 1253, 8000 Bahía Blanca, Argentina
[b] Reaction Kinetics Research Group, Chemical Research Centre of the Hungarian Academy of Sciences, University of Szeged, P.O. Box 168, H-6701 Szeged, Hungary

ARTICLE INFO

Article history:
Received 14 February 2008
Accepted for publication 26 April 2008
Available online 2 June 2008

Keywords:
Carbides
Molybdenum
Density functional calculations
Methanol
Models of surface chemical reactions
Bonding

ABSTRACT

We have studied the adsorption and dissociation of methanol on β-Mo_2C(001) model surface using density functional theory calculations. We modeled the bulk and the Mo-terminated carbide surface using a four layer slab. Methanol is adsorbed with the OH group pointing towards the surface and the formation of the methoxy specie is energetically favorable after H abstraction. The surface outward dipole moment and adsorption heat computed are in agreement with previous experimental data in chemically analogous systems. The bonding analysis using the crystal orbital overlap population (COOP) curves shows a Mo–Mo weakening upon adsorption and a strong H–Mo interaction after dissociation.

1. Introduction

Mo_2C, among other transition metal carbides, presents similar electronic properties to platinum metals and exhibits excellent catalytic behavior in several reactions, accompanied by less sensitivity to sulfur poisoning [1,2]. There are two extensive reviews that have compilated the catalytic properties of these carbides [3,4]. Mo_2C exhibits a unique catalytic property in the aromatization of methane [5–11]. Barthos et al. and Széchenyi et al. [12,13] have reported that Mo_2C on ZSM-5 can markedly enhance the aromatization of ethanol and methanol [12–14]. The adsorption of methanol on Mo_2C has been studied by UHV spectroscopy by Hwu and Chen [15] and the effect of K on the adsorption and dissociation pathway of methanol and ethanol have been reported [16,17]. On other carbides like TiC(100) and VC(100), a fraction of ethanol dissociates at 100 K giving alkoxy intermediates [18]. Then at higher temperatures the alkoxy species are dehydrated to gas phase alkenes.

When Mo_2C is deposited on a carbon support, the reaction pathway of ethanol and methanol is altered and their decomposition to H_2 comes into prominence. In order to obtain more information on the interaction of these alcohols with Mo_2C/Mo(100) surface, several spectroscopy methods have been applied [19–22,16,23].

However, there are still several unsolved questions concerning the adsorption and reactivity of methanol on Mo_2C surfaces. The increasing applicability of modern theoretical methods in various fields of chemistry and catalysis provides an alternative tool to model and understand catalytic reactions at a molecular level.

There are some theoretical studies at density functional theory (DFT) level related to the chemical properties of early transition metal carbide (TMC) surfaces. Kitchin et al. [24] investigated the physical, chemical, electronic structure and hydrogen adsorption on close packed TMC (including Mo_2C(0001) and the surfaces of TiC, VC, NbC and TaC). Their results indicated that H adsorbs more strongly to the metal-terminated carbide surfaces than to the corresponding closest-packed pure metal surfaces. A DFT study for the adsorption of hydrogen on several iron–carbides was published by Cao et al. [25]. Piskorz et al. also reported theoretical studies on Mo_2C surfaces [26] and the K-doping of Mo_2C surfaces has been recently computed by Kotarba et al. using Mo_2C clusters as surface models [27]. Ren et al. [28] have theoretically studied the adsorption of O_2, H and CH_x (x = 0–3) and C_2H_4 on α-Mo_2C(0001). These authors found that CO_2 adsorbs dissociatively into CO and O in agreement with experimental findings. The O, CH_4 and H species prefer the site of three surface molybdenum atoms over a second layer carbon atom.

To the best of our knowledge, there are no studies at DFT level of methanol adsorption on a Mo_2C surface. In the following section we will confirm several experimental data and provide more insight on the adsorption site and about the mechanism for decomposition of methanol to methoxy species.

2. Computational method

The results presented in this paper were obtained with self-consistent DFT calculations using the Vienna Ab Initio Simulation Package (VASP) [29]. This package uses a plane-wave basis and a

* Corresponding author. Tel./fax: +54 291 4595142.
E-mail address: cajuan@uns.edu.ar (A. Juan).

0039-6028/$ - see front matter © 2008 Elsevier B.V. All rights reserved.
doi:10.1016/j.susc.2008.04.039

periodic supercell method. Potentials within the projector-augmeteted wave method (PAW) [30] and the generalized gradient approximation (GGA) with Perdew–Burke–Ernzerhof functional (PBE) [31,32] were used. For bulk optimization, the lattice parameters for β-Mo_2C were determined by minimizing the total energy of the unit cell using a conjugated-gradient algorithm to relax the ions [33]. A $5 \times 5 \times 5$ Monkhorst–Pack k-point grid for sampling the Brillouin zone was considered. Larger sets of k-points were selected ($6 \times 6 \times 6$ and $7 \times 7 \times 7$) making sure that there is no significant change in the calculated energies.

The surface was modeled by four layers slabs separated by vacuum using the DFT lattice parameters previously obtained from bulk optimization. During optimization the first two layers were allowed to fully relax and a set of $3 \times 3 \times 1$ Monkhorst–Pack k-point set was used. Besides, for adsorption calculations the adsorbed species and the first two surface layers were allowed to relax. In all cases, the cutoff energy used was 750 eV.

The adsorption energy was computed by subtracting the energies of the gas phase species and the surface from the energy of the adsorbed system as follows:

$$E_{ads} = E(\text{adsorbate/slab}) - E(\text{adsorbate}) - E(\text{slab})$$

With this definition a negative adsorption energy corresponds to a stable adsorption on the surface.

For a qualitative study on bonding the concept of crystal orbital overlap population (COOP) as implemented in the YAeHMOP code [34] was employed. For this, the optimized geometries previously obtained from DFT were used. A similar procedure was implemented by Papoian et al. [35].

3. Results

3.1. Bulk and surface characterization

3.1.1. Bulk properties

We first tested the parameterization of the DFT method (cutoff energy value, k-point set, smearing function, etc) for the description of the bulk β-Mo_2C. The β-Mo_2C phase has an orthorhombic crystal structure with Mo atoms slightly distorted from their positions in close-packed planes and carbon atoms occupying one-half of the octahedral interstitial sites. In such a way, many reports refer the (0001) plane as a closest-packed surface. The corresponding unit cell is composed by eight molybdenum atoms and four carbon atoms.

The calculated DFT lattice parameters for the bulk β-Mo_2C are $a = 5.273$ Å, $b = 6.029$ Å, $c = 4.775$ Å which are very close to the experimental values ($a = 5.195$ Å, $b = 6.022$ Å, $c = 4.725$ Å) [36]. Our computed value for the bulk modulus was 307.1 GPa in excellent agreement with the experimental data of 307 GPa [37]. Each of the lattice parameters were overestimated in 1–2%. The bulk β-Mo_2C lattice parameters were determined for later use in investigations of supercell properties described in the next section.

The atom projected density of states (PDOS) were calculated by projection of the one-electron states onto spherical harmonic atomic orbitals centered on atomic sites (Fig. 1). PDOS on C and Mo atoms is presented in Fig. 1a. The peak around −12 eV can be attributed to interactions between C s-orbitals with Mo orbitals, while the band between −7 and 2 eV is mainly Mo d-band interacting with C p-band on its lower energy part (between −7 and −4 eV). There is also a strong peak at −27 eV from Mo p-orbitals (out of scale on these figures) which is not relevant for the present analysis.

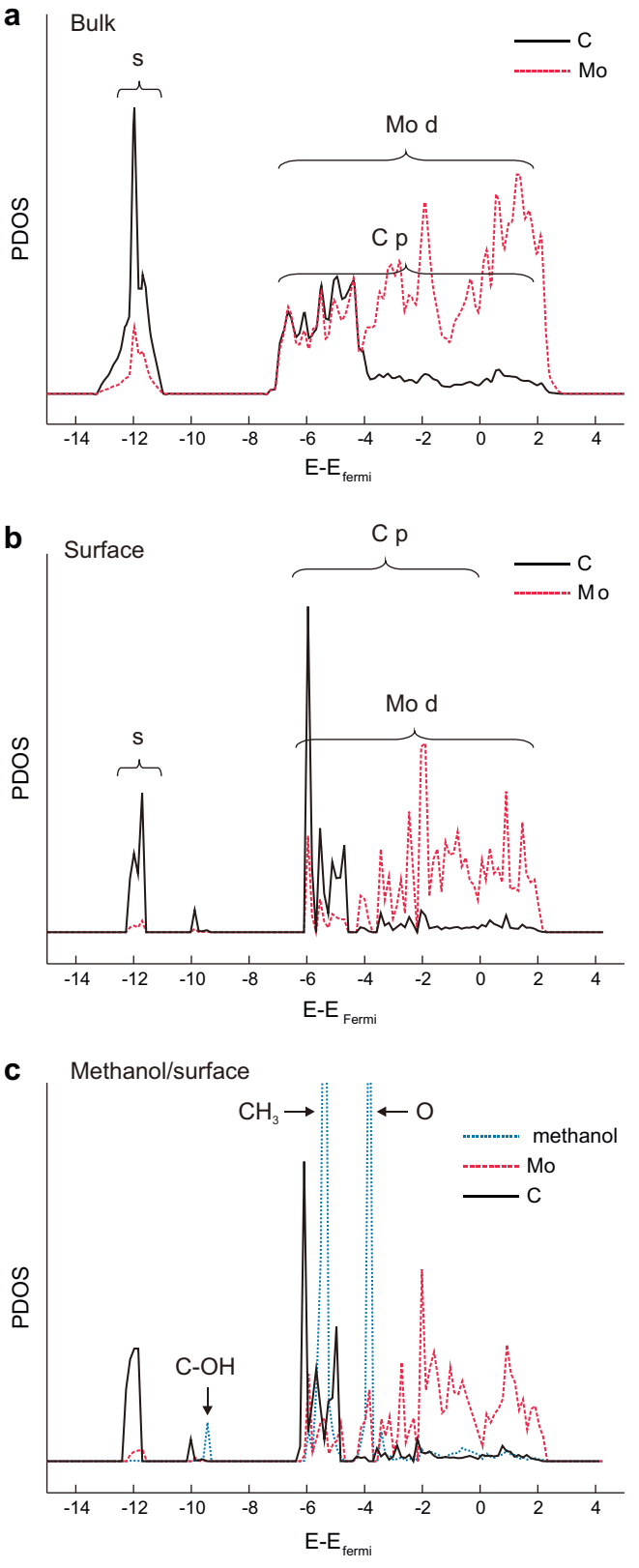

Fig. 1. PDOS on Mo and C atoms for bulk Mo_2C (a), and Mo-terminated surface (b). PDOS on Mo, C and methanol molecule, when methanol is adsorbed on the surface (c).

3.1.2. Surface properties

The structure of β-Mo_2C (001) surface includes a series of alternating Mo and C layers. We modeled the surface with a slab of four layer thickness (two layers of Mo atoms and two layers of C atoms) and each slab has two formula unit cells width. The vacuum spacing between two repeated slabs was 11.8 Å to ensure no significant

interaction between the slabs. During optimization, surface Mo and subsurface C layers were allowed to fully relax while the other two layers were frozen at their bulk lattice parameters. The resulting interlayer distances become shorter than those in the bulk (around 17%).

Projected DOS on surface atoms are shown in Fig. 1b. The new peak at −10 eV is mainly due to the interaction between subsurface C s-orbitals and Mo orbitals. C p-band is narrower and more intense than the corresponding bulk band. The same behavior is observed for the Mo d-band below the Fermi level. Kitchin et al. [24] compared the electronic d band structures of β-Mo_2C (001) surfaces with those of Mo(110) and Pt(111) using DACAPO, they also report similar bands that associates with hybridization between d-orbitals and the carbon s–p orbitals. The locations of the peaks and band widths calculated using DACAPO program are in excellent agreement with our results.

3.2. Methanol adsorption and dissociation

3.2.1. Methanol adsorption

The adsorption of the methanol molecule and its dissociation on H and methoxy specie was investigated using DFT. Previous results for the H adsorption on this surface concludes that H adsorbs more strongly to the metal-terminated carbide surface than to the C-terminated surface [24]. Also Ren et al. [38] found adsorption energies for O and CO 37 and 31% higher on Mo-terminated than on C-terminated surfaces. Mo-terminated surface is very important for catalytic activity and the catalytic reactions occur mainly on it [39–42]. Following this ideas, methanol was adsorbed on a Mo-terminated surface. UHV experimental studies have suggested the presence of methoxy and ethoxy species during methanol or ethanol adsorption and decomposition on the β form of Mo_2C [15–17]. According to this, we have started with the O atom from the methanol molecule pointing towards a Mo-terminated surface. The adsorbate was fully relaxed and so the first two layers of the slab. The final adsorption geometry is shown in Fig. 2. O is finally bonded to a Mo atom on a top position with a O–Mo distance of 2.2 Å and with the H atom pointing towards a 3-fold position. The H–O–CH_3 angle increases by 5%, also O–H and O–C distances increase by 5% and 1% after adsorption. Distances and angles for isolated and adsorbed methanol are indicated in Table 1.

Tables 2 and 3 present the computed charges for the surface and the methanol molecule. The surface withdraws charge from the molecule making it more negative in such a way that the molecule becomes positively charged as a whole, creating a positive outward dipole moment. A similar result was experimentally determined in the case of methanol and ethanol on Mo_2C [15–17] from changes in the work function. When comparing the adsorbed specie with an isolated methanol molecule in vacuum, the H of the OH group also looses some of its orbital occupation reinforcing the idea of charge transference towards the surface. The computed adsorption energy for methanol on Mo_2C results −0.39 eV (−37.8 kJ/mol), which is in excellent agreement with the value of 37 kJ/mol measured from temperature programmed desorption [16]. The subsurface C atoms of the carbide surface do not present any significant change when compared with the clean Mo_2C surface.

Regarding the electronic structure, Fig. 1c shows the PDOS of the adsorbed methanol molecule, the Mo atom bonded to the O of the OH group and the subsurface C of Mo_2C. Two peaks at −5.5 and −4 eV belong to the CH_3 group and to the O atom from the adsorbed methanol, respectively. There is also a small peak at −9.5 eV which also corresponds to the C–OH bond of methanol.

3.2.2. Methanol dissociation to methoxy (first step on methanol reaction on the surface)

According to [16,17], the analysis of the HREEL spectra obtained at 100 K leads to the condition that ethanol adsorbs dissociatively

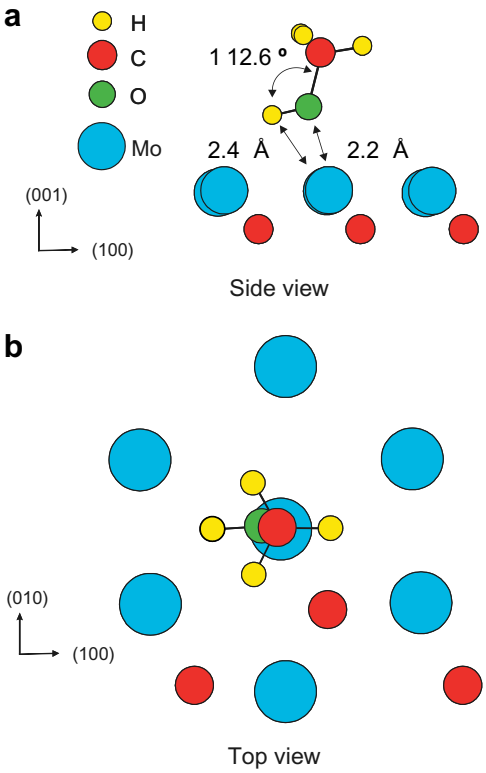

Fig. 2. Surface structure of methanol adsorption on Mo-terminated Mo_2C surface, side (a) and top (b) views. For clarity, not all the surface is shown and only first two layers are included.

Table 1
Calculated geometric parameters for isolated methanol and adsorbed species

		Isolated methanol	Methanol on surface	Methoxy + H on surface
Distance (Å)	C–O	1.42	1.43	1.42
	O–H	0.95	1.00	–
	O–Mo_1	–	2.20	1.98
	H–Mo	–	2.40 (Mo_1)	1.92 (Mo_4)
Angle (°)	COH	106.8	112.6	–

Closest atom distances are indicated and atom labels are indicated in Fig. 3.

Table 2
Net charges for specific atoms on the surface and on isolated and adsorbed species

Charge	Isolated		Methanol on surface	Methoxy + H on surface
	Surface	Methanol		
Mo_1	0.993	–	0.968	0.655
Mo_2	0.866	–	0.852	0.671
Mo_3	0.989	–	0.970	0.726
Mo_4	0.993	–	0.992	0.212
C	−1.252	–	−1.283	−1.283
H(CH_3)	–	−0.050	−0.040	−0.032
H(OH)	–	−0.313	−0.195	0.762
C	–	−1.760	−1.704	−1.715
O	–	2.352	2.348	2.411
			$\Delta q = 0.201$[a]	$\Delta q = 1.233$[a]

Atom labels are indicated in Fig. 3.

[a] The Δq on all the adsorbed species is referenced to an hypothetical charge on an isolated methanol calculated using the same geometrical parameters as in the adsorbate state.

Table 3
Overlap population (OP) for surface bonds

OP		Isolated surface	Methanol on surface	Methoxy + H on surface
Mo–Mo	Mo_1–Mo_2	0.248	0.232	0.236
	Mo_1–Mo_3	0.285	0.269	0.270
	Mo_4–Mo_3	0.280	0.281	0.228
Mo–C	Mo_1–C_5	0.402	0.406	0.401
	Mo_4–C_6	0.409	0.401	0.411
	Mo_2–C_6	0.373	0.369	0.362

Atom labels are indicated in Fig. 3.

on Mo_2C/Mo(100) to yield adsorbed ethoxy and hydrogen $C_2H_5OH(g) \rightarrow C_2H_5OH(ads) \rightarrow C_2H_5O(ads) + H(ads)$. These authors support this idea by the strong evidence for the dissociative adsorption from the absence of the 3260 cm^{-1} peak due to the OH at lower coverages [16]. These experimental results suggested to look for a possible H abstraction from the OH group. Fig. 3 shows a modeled reaction pathway while H is moved away from the methanol to give finally an adsorbed methoxy on top and a H at a 3-fold Mo site. We used a similar methodology to the well known the climbing Nudge Elastic Band (cNEB) method, finding minimum energy position on specific spatial regions to determine this pathway. During this process the energy of the system reduces 0.84 eV for the final state, while there is an activation energy barrier of 0.6 eV The final geometry was fully optimized and the corresponding distances are shown in Table 1.

Concerning the reaction pathway for the dissociation of methanol on Pd(111) there is an agreement that the dehydrogenation to CO and H_2 proceeds via methoxy species. The methoxy is more strongly adsorbed on Mo_2C than methanol. In addition, methoxy becomes closer to surface than adsorbed methanol because the Mo–O distance is reduced by 10%. Mo–H final distances after dissociation are similar to that obtained by Ren [28].

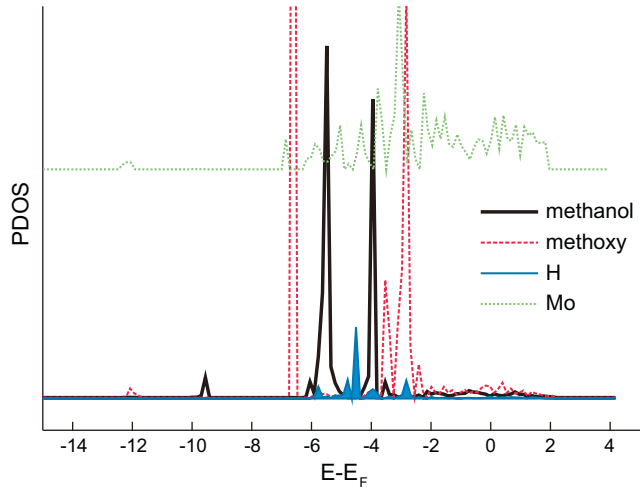

Fig. 4. PDOS on methanol and PDOS on methoxy and H. It is also included PDOS on surface Mo atom bonded to methoxy, shifted upwards.

Table 4
Overlap population (OP) for bonds on isolated methanol and adsorbed species

OP	Isolated methanol	Methanol on surface	Methoxy + H on surface
C–H (CH_3)	0.807	0.779	0.788
C–O	0.536	0.549	0.579
O–H (OH)	0.619	0.642	–
O–Mo	–	0.222	0.463
H–Mo	–	0.015	0.274

In the case of adsorbed H, the charge changes from −0.195 on the adsorbed molecule to +0.762 in the dissociated state. Table 2 presents all the charges during methanol and methoxy formation.

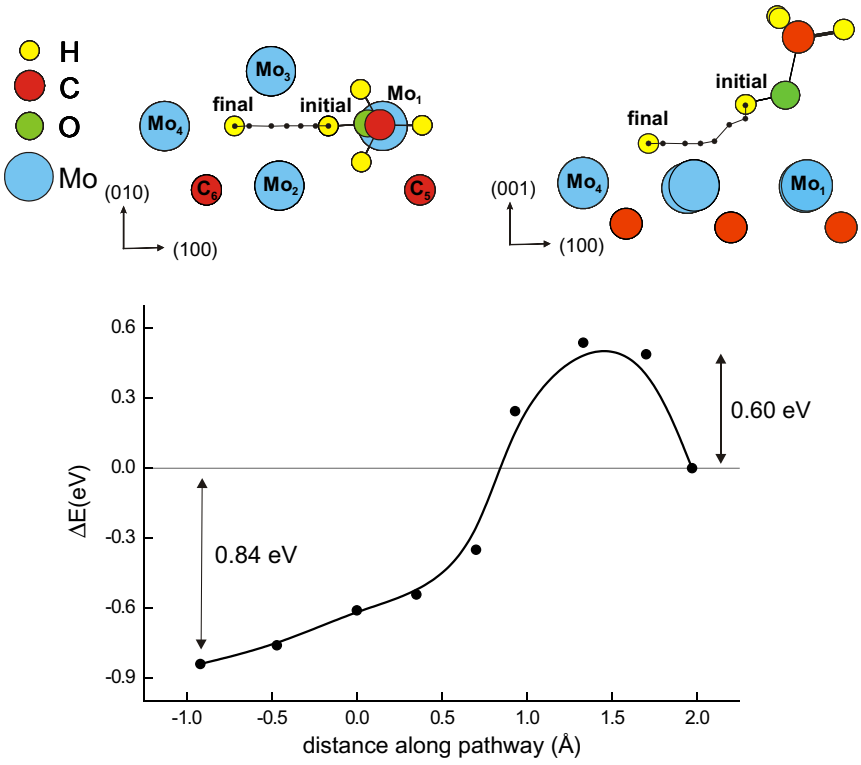

Fig. 3. Reaction pathway and the corresponding energy variation for methanol dissociation from adsorbed methanol (H bonded to the molecule, initial state) to adsorbed methoxy and H (bonded to a surface 3-fold site, final state).

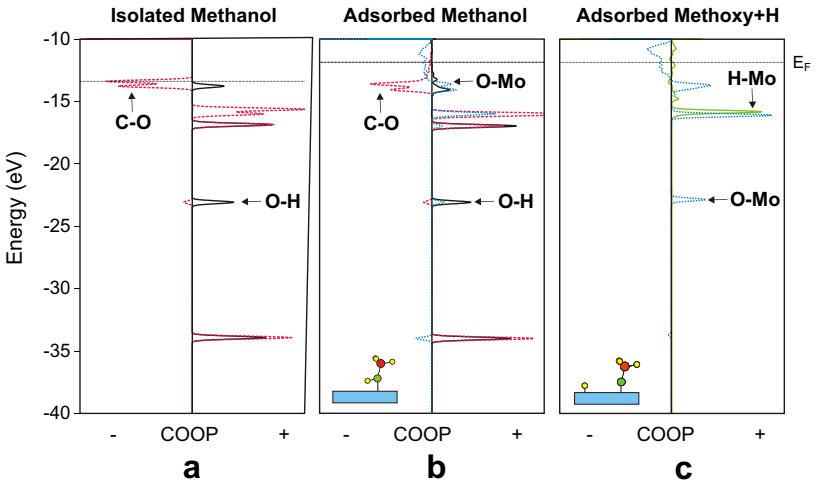

Fig. 5. COOP curves for: C–O and O–H bonds on isolated methanol; for C–O, O–H and O–Mo bonds when methanol is adsorbed on the surface; and for O–Mo and H–Mo bonds when methoxy and H are adsorbed on the surface.

Considering the changes in the electronic structure, PDOS of methanol is compared with PDOS of methoxy + H curves in Fig. 4 (also PDOS on surface Mo bonded to methoxy is presented). The two main peaks from methoxy are further apart from each other than in the case of methanol and the peak at −9.5 eV disappears because it belonged to the OH group. There are also peaks for H between −4 and −5 eV and a new peak at −3 eV interacting in a region where the Mo presents some density of states.

3.2.3. Bonding analysis

The crystal orbital overlap population commonly referred as COOP [43] was used to shed more light on the bonding between methanol, the surface atoms and the methoxy and H species after dissociation.

Table 3 shows the overlap population (OP) for the clean surface, after adsorption and after dissociation. The OP of the Mo–Mo bond decreases upon adsorption while the bulk Mo–C bond remains almost unchanged. When the methoxy group is considered, there is some Mo–Mo bond weakening for the metal bonded to the oxygen from methoxy. However, there is a strong change on the Mo–Mo bond close to the dissociated H form the OH group. In this last case the metal–metal bond wakening is about 20%. The Mo–C bonds close to the H adsorption site present a slight change in bonding of 2%. The changes in the adsorbate OP are presented in Table 4.

The C–H bond from CH_3 group presents slight changes during adsorption and reaction (a 3% decrease). There is an initial reinforcement of the OH bond upon adsorption. There also appears an OP for the O–Mo interaction which is increased more than 100% when the methoxy specie is formed. There is also an OP value for the H–Mo interaction when methanol is adsorbed, which increases significantly when H is finally dissociated.

Fig. 5 shows the COOP curves for the OH and CO bonds of methanol before and after adsorption. It can be seen than the peaks around −16 eV after adsorption increase its bonding contribution while the peaks at −14 eV decrease its antibonding contribution for the C–O bond.

Fig. 5 also shows the COOP curve the Mo–O bond. Finally in the case of methoxy + H, the COOP curves show Mo–O bonding contributions and a strong H–Mo bonding peak at −15 eV.

4. Conclusions

The adsorption of methanol and the first step on its dissociation on β-Mo_2C(001) surface have been computed. The methanol adsorption results to be a favorable process on a Mo-terminated surface with an adsorption energy of −37.8 kJ/mol, which is very close to the experimental value.

Regarding the bonding, the methanol was found positioned with the O atom towards the surface in a close a-top position with a O–Mo distance of 2.2 Å and with the H atom pointing towards a 3-fold position.

Besides, the surface withdraws charge from the molecule, creating a positive outward dipole moment as previously determined by work function changes.

The dissociation to a methoxy specie is energetically favorable although there is an activation energy barrier and our results support the idea of H abstraction from the OH group.

Considering the changes in the bonding, the Mo–Mo bond strength decreases when methanol is adsorbed. When the methoxy is formed, the Mo–O contribution is bonding and a strong H–Mo peak is clearly seen.

Finally, calculations show an excellent agreement with previous data for methanol on β-Mo_2C [15–17] and our results compare very well in the case of methanol and ethanol due to their chemical similarity.

Acknowledgements

The authors thank the SGCyT-UNS, CONICET and SECyT-Argentina/NK TH-Hungary for their financial support. A. Juan and C. Pistonesi are members of CONICET. Stimulating discussion with L. Óvári, T. Bánsági and L. Bugyi are also acknowledged.

References

[1] S.T. Oyama, Catal. Today 15 (22) (1992) 179.
[2] S.T. Oyama, The Chemistry of Transition Metal Carbides and Nitrides, Blakie Academia and Professional, Waisan, Poland, 1996.
[3] J.G. Chen, Chem. Rev. 96 (1996) 1477.
[4] H.H. Hwu, J.G. Chen, Chem. Rev. 105 (2005) 185.
[5] D.W. Wang, J.H. Lunsford, M.P. Rosynek, Top. Catal. 3 (4) (1996) 299.
[6] F. Solymosi, A. Szőke, J. Cserényi, Catal. Lett. 39 (1996) 157.
[7] F. Solymosi, J. Cserényi, A. Szőke, T. Bánsági, A. Oszkó, J. Catal. 165 (1997) 150.
[8] D.W. Wang, J.H. Lunsford, M.P. Rosynek, J. Catal. 169 (1997) 347.
[9] R.W. Borry III, E.C. Lu, K. Young-ho, E. Iglesia, Stud. Surf. Sci. Catal. 119 (1998) 403.
[10] L.S. Liu, L. Wang, R. Ohnishi, M.J. Ichikawa, J. Catal. 181 (1999) 175.
[11] J.-Z. Zhang, M.A. Long, R.F. Howe, Catal. Today 44 (1998) 293.
[12] A. Széchenyi, R. Barthos, F. Solymosi, Catal. Lett. 110 (2006) 85.
[13] R. Barthos, A. Széchenyi, F. Solymosi, J. Phys. Chem. B 110 (2006) 21816.
[14] R. Barthos, T. Bánsági, T. Sülizakar, F. Solymosi, J. Catal. 247 (2007) 368.

[15] H.H. Hwu, J.G. Chen, Surf. Sci. 536 (2003) 75.
[16] A.P. Farkas, F. Solymosi, Surf. Sci. 601 (2007) 193.
[17] A.P. Farkas, F. Solymosi, Surf. Sci. 602 (2008) 1475.
[18] R.L. Guenard, L.C. Fernández-Torres, B.-I. Kim, S.S. Perry, P. Frantz, S.V. Didziulis, Surf. Sci. 515 (2002) 103.
[19] R. Barthos, A. Szechenyi, A. Koos, F. Solymosi, Appl. Catal. A: Gen. 327 (2007) 95.
[20] A. Szechenyi, F. Solymosi, J. Phys. Chem. C 111 (2007) 9509.
[21] R. Barthos, F. Solymosi, J. Catal. 249 (2007) 289.
[22] E.I. Ko, R.J. Madix, Surf. Sci. 112 (1981) 373.
[23] A.P. Farkas, Ph.D. Thesis, University of Szeged, 2007.
[24] J.R. Kitchin, J.K. Norskov, M.A. Barteau, J.G. Chen, Catal. Today 105 (2005) 66.
[25] D.B. Cao, F.Q. Zhang, Y.W. Li, J.G. Wang, H. Jiao, J. Phys. Chem. B 109 (2005) 833.
[26] W. Piskorz, G. Adamski, A. Kotarba, Z. Sojka, C. Sayag, G. Djéga-Mariadassou, Catal. Today 119 (2007) 39.
[27] A. Kotarba, G. Adamski, W. Piskorz, Z. Sojka, C. Sayag, G. Djéga-Mariadassou, J. Phys. Chem. B 108 (2004) 2885.
[28] J. Ren, C. Huo, J. Wang, Z. Cao, Y. Li, H. Jiao, Surf. Sci. 600 (2006) 2329.
[29] G. Kresse, J. Furthmller. <http://cms.mpi.univie.ac.at/vasp/vasp/vasp.html>.
[30] G. Kresse, D. Joubert, Phys. Rev. B 59 (1999) 1758.
[31] J.P. Perdew, K. Burke, M. Ernzerhof, Phys. Rev. Lett. 77 (1996) 3865.
[32] J.P. Perdew, K. Burke, M. Ernzerhof, Phys. Rev. Lett. 78 (1997) 1396.
[33] W.H. Press, B.P. Flannery, S.A. Teukolsky, W.T. Vetterling, Numerical Recipies, Cambridge University Press, New York, 1986.
[34] G. Landrum, W. Glassey, Yet Another Extended Hückel Molecular Orbital Package (YAeHMOP), Cornell University, 1997. <http://yaehmop.sourceforge.net>.
[35] G. Papoian, J. Norskov, R. Hoffmann, J. Am. Chem. Soc. 122 (2000) 4129.
[36] E. Parthé, V. Sadagopan, Acta Cryst. 16 (1963) 202.
[37] J. Haines, J. Léger, C. Chateau, J. Lowther, J. Phys. Condens. Matter 13 (2001) 2447.
[38] J. Ren, C. Huo, J. Wang, Y. Li, H. Jiao, Surf. Sci. 596 (2005) 212.
[39] S.T. Oyama, C.C. Yu, S. Ramanathan, J. Catal. 184 (1999) 35.
[40] J.A. Rodriguez, J. Dvorak, T. Jirsk, Surf. Sci. 457 (2000) L413.
[41] T.E. Lucy, T.P.St. Clair , S.T. Oyama, J. Mater. Res. 13 (1998) 2321.
[42] V. Schwartz, V.T. DaSilva, S.T. Oyama, J. Mol. Catal. A 163 (2000) 251.
[43] R. Hoffmann, Solids and Surfaces: A Chemist's View of Bonding in Extended Structures, VCH Publishers, New York, 1988.